FEBS Letters 473 (2000) 58–62 FEBS 23632

Detection of superoxide anion using an isotopically labeled nitrone spin trap: potential biological applications

Hao Zhang[a], Joy Joseph[a], Jeannette Vasquez-Vivar[b], Hakim Karoui[c], Cline Nsanzumuhire[c], Pavel Martásek[d], Paul Tordo[c], B. Kalyanaraman[a,*]

[a] *Biophysics Research Institute, Medical College of Wisconsin, 8701 Watertown Plank Road, Milwaukee, WI 53226, USA*
[b] *Department of Pathology and Cardiovascular Research Center, Medical College of Wisconsin, Milwaukee, WI, USA*
[c] *Laboratoire 'Structure et Réactivité des Espèces Paramagnétiques', Université de Provence, Marseille, France*
[d] *University of Texas Health Sciences Center, San Antonio, TX, USA*

Received 30 March 2000

Edited by Barry Halliwell

Abstract We describe the synthesis and biological applications of a novel nitrogen-15-labeled nitrone spin trap, 5-ethoxycarbonyl-5-methyl-1-pyrroline *N*-oxide ([^{15}N]EMPO) for detecting superoxide anion. Superoxide anion generated in xanthine/xanthine oxidase (100 nM min^{-1}) and NADPH/calcium-calmodulin/nitric oxide synthase systems was readily detected using EMPO, a nitrone analog of 5,5′-dimethyl-1-pyrroline *N*-oxide (DMPO). Unlike DMPO-superoxide adduct (DMPO–OOH), the superoxide adduct of EMPO (EMPO–OOH) does not spontaneously decay to the corresponding hydroxyl adduct, making spectral interpretation less confounding. Although the superoxide adduct of 5-(diethoxyphosphoryl)-5-methyl-pyrroline *N*-oxide is more persistent than EMPO–OOH, the electron spin resonance spectra of [^{14}N]EMPO–OOH and [^{15}N]EMPO–OOH are less complex and easier to interpret. Potential uses of [^{15}N]EMPO in elucidating the mechanism of superoxide formation from nitric oxide synthases, and in ischemia/reperfusion injury are discussed.

Key words: Electron spin resonance; Spin trap; Nitric oxide synthase; Vascular biology; Tetrahydrobiopterin

1. Introduction

There is a surge of research interest in the development of more effective and selective probes to detect superoxide anion generated in enzymatic and cellular systems and perfused organs [1–3]. Current assays for superoxide rely on the measurement of cytochrome *c* reduction, chemiluminescence from lucigenin and related dyes, nitro blue tetrazolium reduction to formazan, dihydroethidium oxidation to ethidium, aconitase inactivation/activation, or electron spin resonance (ESR) spin-trapping. However, nearly all of these assays have been criticized for various reasons [4–9]. We have undertaken this study to improve the existing spin-trapping methodology for detecting superoxide anion in biological systems.

5,5-Dimethyl-pyrroline *N*-oxide (DMPO) has been used for decades to trap superoxide anion in biological systems [10]. A major disadvantage of DMPO is that the DMPO-superoxide adduct (DMPO–OOH) spontaneously decays to the DMPO–hydroxyl adduct (DMPO–OH) and as a result, superoxide anion was typically detected by monitoring the superoxide dismutase-inhibitable formation of DMPO–OH. This potential drawback was recently overcome with the synthesis of a phosphorylated analog, 5-(dimethoxyphosphoryl)-5′-methyl-1-pyrroline *N*-oxide (DEPMPO) [11]. In contrast to DMPO–OOH, the DEPMPO-superoxide adduct (DEPMPO–OOH) does not decompose to the DEPMPO–hydroxyl adduct (DEPMPO–OH) [10,11]. Despite the stability of DEPMPO–OOH, the use of DEPMPO in superoxide spin-trapping remains limited in biological systems because the ESR spectra of DEPMPO adducts are complicated by an additional ^{31}P hyperfine coupling and the existence of diastereomers. Substitution of the 5-methyl group with an electron-withdrawing β-ethoxyphosphoryl group increased the stability of DEPMPO–OOH and led to the synthesis of a carboxylated analog, 5-ethoxycarbonyl-5-methyl-pyrroline *N*-oxide (EMPO) [12,13]. The EMPO superoxide adduct (EMPO–OOH) was reported to be eight times more stable than DMPO–OOH. In addition, EMPO–OOH exhibits an ESR spectrum that is very similar to that of DMPO–OOH. In this work, we show that the signal-to-noise ratio of the ESR spectrum of EMPO–OOH is further enhanced by labeling the nitrone group in EMPO with a nitrogen-15 atom. We also discuss the use of [^{15}N]EMPO in the elucidation of the mechanism of superoxide generation from endothelial and neuronal nitric oxide synthases (eNOS and nNOS) and its implications in vascular dysfunction.

2. Materials and methods

2.1. Materials

All chemicals were purchased from Sigma-Aldrich and used as received.

2.2. Methods

2.2.1. Synthesis of [^{15}N]EMPO. [^{15}N]EMPO was synthesized from the precursor compound, [^{15}N]nitro ethyl propionate, which was prepared as follows [14,15]. Ethyl 2-bromopropionate (5.85 g, 0.03 mol) was added while stirring to a mixture of 60 ml anhydrous

*Corresponding author. Fax: (1)-414-456 6512.
E-mail: balarama@mcw.edu

Abbreviations: ESR, electron spin resonance; DMPO, 5,5-dimethyl-1-pyrroline *N*-oxide; DEPMPO, 5-(dimethoxyphosphoryl)-5′-methyl-1-pyrroline *N*-oxide; EMPO, 5-ethoxycarbonyl-5-methyl-pyrroline *N*-oxide; nNOS, neuronal nitric oxide synthase; eNOS, endothelial nitric oxide synthase; DMPO–OOH, DMPO superoxide adduct; DEPMPO–OOH, DEPMPO superoxide adduct; EMPO–OOH, EMPO superoxide adduct; EMPO–OH, EMPO hydroxyl adduct

PII: S0014-5793(00)01498-8

dimethylformamide containing [^{15}N]sodium nitrite (3.6 g, 0.05 mol) and phloroglucinol dihydrate (4.0 g, 0.052 mol). The reaction was continued at 25°C for 2.5 h. The deep brown reaction mixture was subsequently poured into 120 ml ice-cold water and extracted with ether (4×50 ml). The combined ether extract was washed with 50 ml saturated sodium bicarbonate solution, dried, and the ether removed in a rotary evaporator. The residual yellow liquid was distilled (boiling point 80°C at 10 mm Hg pressure) to give a net yield of 3.2 g (41%) [^{15}N]2-nitro ethyl propionate, which was used in the synthesis of [^{15}N]2-ethoxycarbonyl-2-nitro pentanal.

Ethyl 2-nitropropionate (3.2 g) was added to a sodium ethoxide solution (prepared by reacting 0.1 g metallic sodium in 20 ml dry ethanol), followed by the addition of 1.5 ml acrolein. The mixture was refluxed at 40–50°C for 3 h, acidified with 0.2 ml acetic acid, and extracted with 50 ml dry ether. The ether extract containing the product was passed through a silica gel column and eluted with a 3:1 mixture of hexane:ethyl acetate. Removal of the solvent yielded 3.1 g (70%) [^{15}N]2-ethoxycarbonyl-2-nitro pentanal. This aldehyde product was converted to a 1:3 dioxolan derivative by refluxing in 25 ml benzene containing ethylene glycol (3 g) and *p*-toluene sulfonic acid (50 mg) with the concomitant removal of water. The benzene solution of 1:3 dioxolan was diluted with 50 ml ether and washed with H_2O (40 ml) and saturated sodium bicarbonate (40 ml). The solvent was removed in a rotary evaporator and the pure dioxolan derivative (3 g, 80% yield) was isolated by distillation (boiling point 121–125°C at 0.5 mm Hg pressure).

The dioxolan derivative was reduced with zinc dust (4 g) in 50% aqueous ethanol (25 ml) containing ammonium chloride (0.6 g) at 5–10°C. After stirring for 2.5 h, the mixture was filtered and the filtrate was concentrated and extracted with 4×25 ml chloroform. The chloroform extract was dried and evaporated to yield a viscous oil of the hydroxylamine. This hydroxylamine product was treated with 50 ml 0.3 N HCl and kept at room temperature for complete hydrolysis and liberation of the aldehyde. To this acid solution 10 ml concentrated ammonia solution was added and extracted with 4×25 ml chloroform after saturating with sodium borate. The chloroform extract was dried and the solvent removed to obtain a yellow oil. Distillation of the yellow oil at 120°C and 0.3 mm Hg pressure yielded 1.1 g (52%) [^{15}N]EMPO, which was obtained as a colorless oil. The [^{14}N] analog of EMPO was prepared in a similar manner, starting from commercially available [^{14}N]2-nitro-ethyl propionate.

2.2.2. nNOS activity. nNOS activity was determined by quantifying the conversion of L-[^{14}C]arginine to L-[^{14}C]citrulline as described previously [16]. Briefly, nNOS (66.7 nM) was added to reaction mixtures (final volume, 0.20 ml) containing HEPES (50 mM, pH 7.4), diethylenetriamine penta-acetic acid (DTPA) (100 μM), L-[^{14}C]arginine (0.1 mM, 0.625 μCi), NADPH (0.3–0.5 mM), calcium chloride (0.2 mM), calmodulin (20 μg ml^{-1}), tetrahydrobiopterin (BH_4) (10 μM), reduced glutathione (100 μM), and bovine serum albumin (200 μg ml^{-1}). To stop the reaction, an aliquot of the reaction mixture (50 μl) was diluted in HEPES (50 mM, pH 5.5) containing EGTA (0.5 mM) and chilled on ice. L-[^{14}C]Citrulline was isolated from the excess of L-[^{14}C]arginine using a Dowex 50W-cation exchange column, and its concentration was determined by liquid scintillation counting.

2.2.3. Xanthine oxidase activity. Xanthine oxidase was incubated with xanthine (1 mM) in phosphate buffer (100 mM) containing DTPA (100 μM). Formation of uric acid was monitored at 296 nm using the extinction coefficient of 11 000 M^{-1} cm^{-1}. Because of interference with uric acid absorption, EMPO was excluded in optical measurements.

2.2.4. ESR measurements. ESR spectra were recorded at room temperature on a Varian E-109 spectrometer operating at 9.03 GHz and 100 kHz field modulation equipped with a TE_{102} cavity or a loop-gap resonator [17,18]. Typical spectrometer parameters were: microwave power, 2 mW; modulation amplitude, 1 G; time constant, 0.064 s; scan rate, 1.67 G s^{-1}; number of scans, three unless otherwise specified. nNOS was added to incubation mixtures (20 μl, final volume) containing [^{14}N]EMPO or [^{15}N]EMPO, and the sample was examined after incubation for 1 min. Data were collected using the VIKING software program developed at the Medical College of Wisconsin, and simulated with the ESR software developed by Rockenbauer [19] and Duling from the Laboratory of Molecular Biophysics at the National Institute of Environmental Health Sciences, Research Triangle Park, NC, USA.

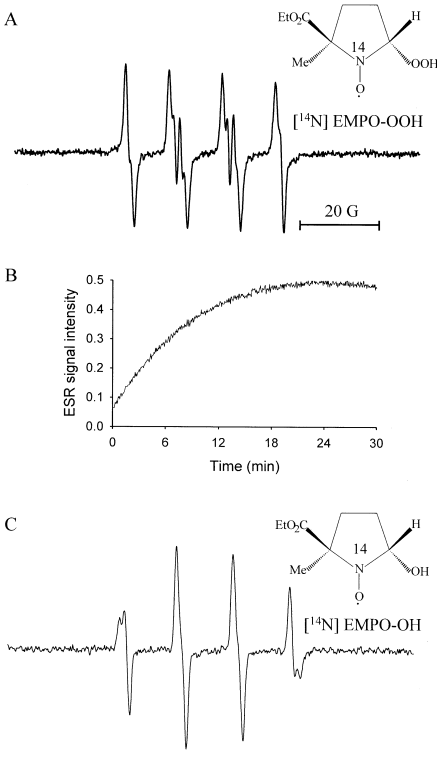

Fig. 1. Trapping of superoxide and hydroxyl radical by [^{14}N]EMPO, formed in the xanthine/xanthine system. A: Incubation mixtures contained xanthine (1 mM), [^{14}N]EMPO (25 mM), DTPA (100 μM), and xanthine oxidase (0.05 U ml^{-1}) in phosphate buffer (100 mM, pH 7.4). The reaction was initiated by the addition of xanthine oxidase, and the steady-state ESR spectrum was recorded after 15 min. B: Time-dependent increase in the formation of EMPO–OOH. The low-field line was monitored as a function of time. Incubation conditions were identical to those described above. C: Incubation conditions are the same as (A) except the mixture contained Fe(III)–EDTA (100 μM) instead of DTPA.

3. Results

3.1. Trapping of superoxide anion by [^{14}N]EMPO and [^{15}N]EMPO

Fig. 1A shows the ESR spectrum, characteristic of [^{14}N]EMPO–OOH, generated from the addition of xanthine oxidase to aerobic incubations containing xanthine (1 mM), [^{14}N]EMPO (25 mM), and DTPA (100 μM) in phosphate buffer (100 mM, pH 7.4). The ESR signal growth of [^{14}N]EMPO–OOH as a function of time is shown in Fig. 1B. The steady-state ESR spectrum was maintained for up to 20 min under these experimental conditions. In the presence of Fe–EDTA, addition of xanthine oxidase to incubations containing xanthine (1 mM) and [^{14}N]EMPO (25 mM) produced the EMPO–OH adduct with a distinctly different ESR spectrum (Fig. 1C).

Fig. 2A–C shows the ESR spectra of [^{14}N]EMPO–OOH, [^{15}N]EMPO–OOH, and [^{14}N]EMPO–OH generated in the xanthine/xanthine oxidase system. Based on computer simulations (dotted-line spectra), these spectra were assigned to a mixture of two diastereomers. In the case of superoxide adducts, spectra 2A and 2B were simulated assuming the presence of two conformers undergoing a chemical exchange [19] (Table 1).

To determine whether [^{14}N]EMPO–OOH decays to form

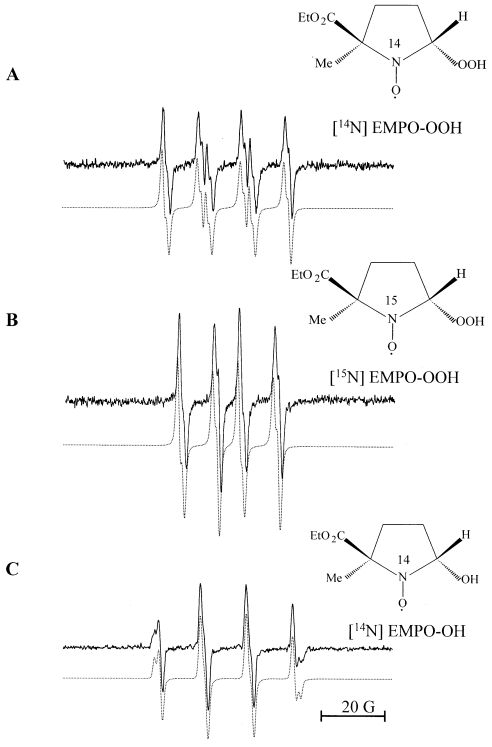

Fig. 2. Computer simulations of [^{14}N]EMPO–OOH, [^{15}N]EMPO–OOH, and [^{14}N]EMPO–OH. ESR spectra of these adducts were obtained in xanthine/xanthine oxidase systems. Dotted lines indicate the computer simulations using the parameters shown in Table 1.

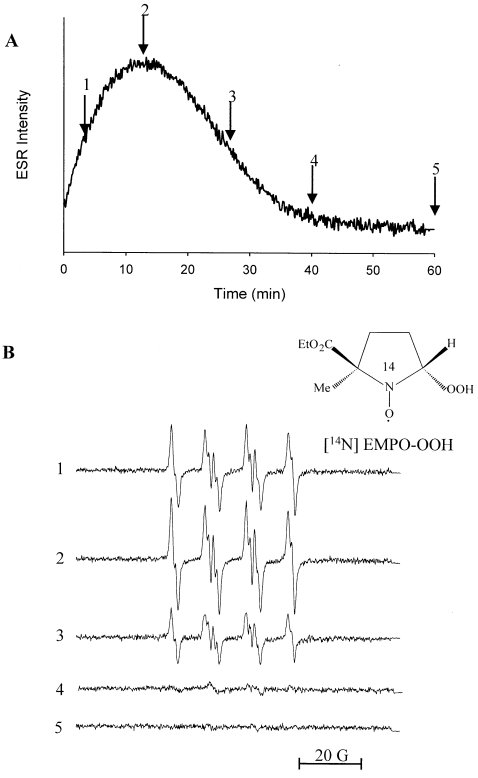

Fig. 3. Time-dependent changes in ESR spectra of EMPO–OOH. A: The low-field line of EMPO–OOH was monitored as a function of time. Incubation conditions are the same as described in Fig. 1 except for xanthine oxidase (0.1 U ml^{-1}). B: At various time points (marked by downward arrows), two steady-state ESR spectra were observed. Spectra 1–5 were recorded at 5, 12, 20, 40, and 60 min after starting the incubation. Note that EMPO–OOH does not decay to EMPO–OH.

other free radical adducts, we monitored the ESR spectra (Fig. 3B) at different time points in xanthine/xanthine oxidase incubations as indicated in Fig. 3A. In these spectra, no additional ESR signal was detected with decreasing signal intensity from decaying [^{14}N]EMPO–OOH. This pattern is clearly different from that of DMPO–OOH, which decayed to form DMPO–OH. These results suggest that if the EMPO–OH spectrum is detected, it is more likely to be formed from trapping of hydroxyl radicals or by another mechanism than from the decomposition of EMPO–OOH.

Next we evaluated the sensitivity of trapping superoxide by [^{14}N]EMPO and [^{15}N]EMPO. Fig. 4A shows the rates of uric acid formation (9.27 ± 0.07; 0.84 ± 0.07, and 0.11 ± 0.01 μM min^{-1}) from three different xanthine oxidase concentrations. The same incubations containing [^{14}N]EMPO and [^{15}N]EMPO were used for ESR measurements. At the indicated time points, the ESR spectra of [^{14}N]EMPO–OOH (Fig. 4B) and [^{15}N]EMPO (Fig. 4C) were recorded. The steady-state EMPO–OOH spectrum can be easily detected at rates of superoxide anion formation ($\cong$100 nM min^{-1}). A comparison of Fig. 4B and C shows that under a wide range of superoxide anion generation rates, the signal-to-noise ratio of [^{15}N]EMPO–OOH was significantly higher than that of [^{14}N]EMPO–OOH.

3.2. EMPO spin-trapping of superoxide anion generated by nitric oxide synthase

Fig. 5 shows the ESR spectra of [^{14}N]EMPO–OOH and [^{15}N]EMPO–OOH formed from the addition of BH_4-free nNOS to incubations containing NADPH (100 μM), Ca^{2+} (0.2 mM)/calmodulin (20 μg ml^{-1}), and EMPO (50 mM). EMPO (50 mM) did not affect the NOS activity as measured by formation of L-citrulline (213 ± 15 nmol min^{-1} (mg protein)$^{-1}$). The signal-to-noise ratio of the superoxide adduct obtained with the [^{15}N]EMPO trap is significantly higher than that obtained with [^{14}N]EMPO (Fig. 5A,B). In the absence of

Table 1
ESR hyperfine coupling constants for superoxide and hydroxyl spin adducts of EMPO

Spin adduct	Diastereomers (%)	Hyperfine coupling constant (G)			Exchange rate (ns)
		a_N	a_H^β	a_H^γ	
[^{14}N]EMPO–OH	52	13.5	14.8	0.8	–
	48	13.5	12.4	–	
[^{14}N]EMPO–OOH	54	12.8	12.1	0.15	130
	46	12.8	8.6	–	
[^{15}N]EMPO–OOH	55	17.9	12.0	0.3	140
	45	17.8	8.7	–	

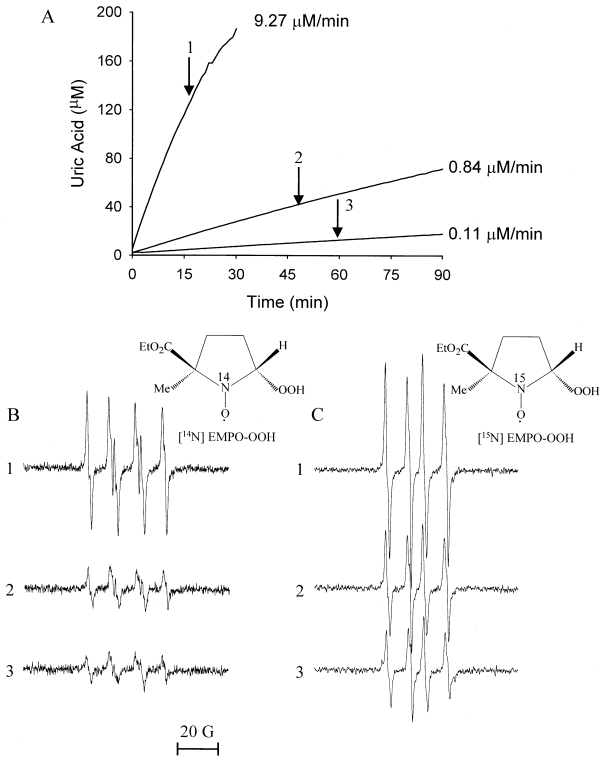

Fig. 4. Spin-trapping of superoxide anion produced at different rates in the xanthine/xanthine oxidase system: effect of [^{15}N]-substitution on spectral resolution. A: Incubation mixtures contained xanthine (1 mM), DTPA (100 μM), and xanthine oxidase (0.5, 0.005, or 0.0005 U ml^{-1}) for optical measurements. For ESR measurements, incubation mixtures were identical except [^{14}N]EMPO or [^{15}N]EMPO (25 mM) was included. Formation of uric acid was measured as shown in these traces. B: At different time points (1, 2, and 3) indicated by a downward arrow, the incubation mixture was transferred to an ESR capillary and the steady-state ESR spectra were recorded. Traces 1, 2, and 3 indicate the EMPO–OOH spectrum detected in the incubation mixtures. C: Same as (B) except that the incubation mixtures contain [^{15}N]EMPO instead of [^{14}N]EMPO.

Ca^{2+}/calmodulin, no ESR spectrum was obtained, indicating that NOS activation was required to produce superoxide anions (Fig. 5C). Real-time measurements of superoxide released from eNOS and inducible NOS were made possible using [^{15}N]EMPO (data not shown).

4. Discussion

4.1. Resolution enhancement caused by ^{15}N-labeling

The ESR spectrum of [^{15}N]EMPO–OOH consists of four lines, compared to six lines detected for [^{14}N]EMPO–OOH. The four-line pattern arises from the interaction of an unpaired electron with a ^{15}N atom ($I = 1/2$) and a β-hydrogen ($I = 1/2$). The ratio of hyperfine coupling between ^{14}N and ^{15}N was calculated to be equal to the gyromagnetic ratio of ^{14}N and ^{15}N magnetic moments (i.e. 0.7).

Although [^{15}N]-substituted DMPO improved the signal-to-noise ratio of DMPO–OOH and DMPO–OH, the [^{15}N]DMPO–OOH also decays to [^{15}N]DMPO–OH. Thus [^{15}N]-substitution of DMPO did not remove this artifact. In contrast, [^{15}N]-substitution in EMPO has the added advantage of increased stability of the [^{15}N]EMPO–OOH adduct (as compared to the [^{15}N]DMPO–OOH), coupled with increased spectral resolution. These features make [^{15}N]EMPO an ideal spin trap for detecting superoxide in biological systems.

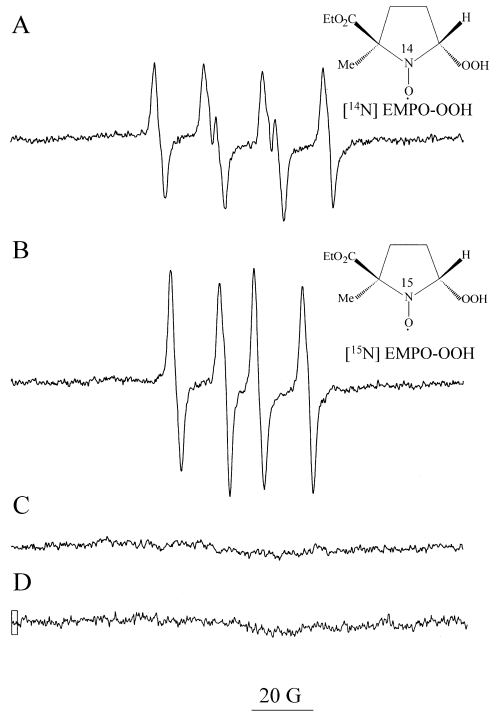

Fig. 5. Trapping of superoxide anion by [^{14}N]EMPO and [^{15}N]EMPO, formed from neuronal nitric oxide synthase. A: Incubations contained NADPH (0.5 mM), [^{14}N]EMPO (25 mM), calcium (0.2 mM), calmodulin (20 μg ml^{-1}), DTPA (100 μM), and purified nNOS (1 μM) in HEPES buffer (50 mM, pH 7.4). B: Same as (A) but in the presence of [^{15}N]EMPO (25 mM). C: Same as (A) but containing superoxide dismutase (10 μg ml^{-1}). D: Same as (A) but in the absence of Ca^{2+}/calmodulin. ESR spectra were obtained after 1 min following the addition of nNOS.

4.2. Relative stability of cyclic nitrone superoxide adducts

Fig. 6 shows the relative half-lives of different superoxide adducts of DMPO, DEPMPO, EMPO, and analogs. Substitution of one of the methyl groups (at the C-5 position) in DMPO with a strong electron-withdrawing diethoxyphos-

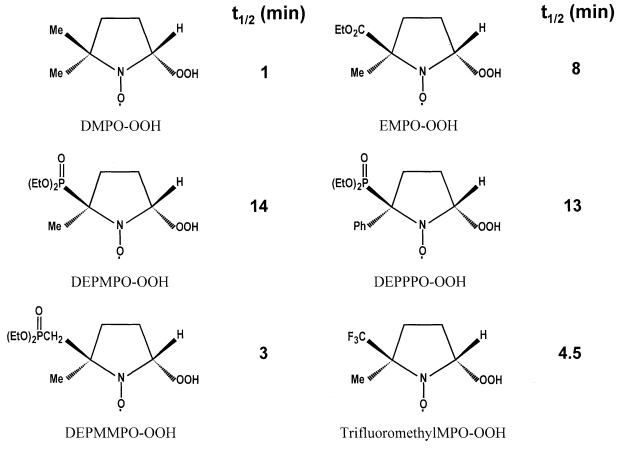

Fig. 6. Relative half-lives of different superoxide spin adducts. (Taken from [12,20–22]).

phoryl group resulted in the greatest stabilization of the corresponding superoxide adduct [20,21]. For example, the half-life of DEPMPO–OOH is 14 times longer than that of DMPO–OOH. When a methylene spacer was inserted between the phosphoryl group and the C-5 atom, the half-life of the resulting superoxide adduct was diminished almost five times [20]. EMPO–OOH, which has an electron-withdrawing carboxyethyl group, has a half-life of 8 min. In addition to the electron-withdrawing effect, it appears that the relative size of the substituent also plays a key role in the stabilization of the superoxide adduct [22].

4.3. Potential biological applications

Increasing evidence suggests that enhanced generation of superoxide anion plays a key role in endothelial dysfunction and associated vascular pathologies [23,24]. It has been proposed that eNOS can regulate both nitric oxide and superoxide anion formation in the vasculature [25,26]. BH_4, a critical cofactor of all NOS enzymes, regulates nitric oxide and superoxide anion formation from NOS [27]. In the absence of BH_4 or under limited availability of BH_4, NOS enzyme becomes 'uncoupled', leading to superoxide formation at the oxygenase domain [28]. ESR spin-trapping provided the first evidence for formation of superoxide anion from purified eNOS and nNOS under conditions of BH_4 deficiency [16,17]. As NOS flavin semiquinone can directly reduce cytochrome *c* (acetylated and succinylated) and BH_4 itself can reduce cytochrome *c* by a mechanism independent of superoxide dismutase, superoxide formation from NOS cannot be reliably measured by cytochrome *c* reduction [6,16,17]. Spin-trapping is ideally suited for detecting superoxide formed in these systems. Spin-trapping with [^{15}N]EMPO should help unravel the role of arginine, NOS inhibitors, and BH_4 in regulating superoxide formation from NOS.

[^{15}N]EMPO may be useful in the detection of superoxide during ischemia/reperfusion. DEPMPO spin-trapping provided the first spectroscopic evidence for superoxide formation in ischemia/reperfusion of isolated rat myocardium [3,11]. Because of the availability of pure [^{15}N]EMPO, increased stability of [^{15}N]EMPO–OOH, and improved signal-to-noise ratio, EMPO spin-trapping of superoxide is likely to have a much broader application in cardiovascular and neurodegenerative pathologies.

In summary, we conclude that the increased stability of ^{15}N-labeled EMPO superoxide adduct coupled with its enhanced spectral resolution should make this nitrone trap ideal for detecting and quantitating superoxide anion formed from NOS enzymes and other oxidases in vascular and neuronal tissues.

Acknowledgements: This work was supported by Grants from the National Institutes of Health (HL47250, HL63119, CA77822, HL61414, and RR01008), and by Grant-in-Aid #9950629N from the American Heart Association to J.V.

References

[1] Tarpey, M.M., White, R.C., Suarez, E., Richardson, G., Radi, R. and Freeman, B. (1999) Circ. Res. 84, 1203–1211.
[2] Dikalov, S., Grigor'ev, I.A., Voinov, M. and Bassenge, E. (1998) Arch. Biochem. Biophys. 248, 211–215.
[3] Fréjaville, C., Karoui, H., Tuccio, B., Le Moigne, F., Culcasi, M., Pietri, S., Lauricella, R. and Tordo, P. (1995) J. Med. Chem. 38, 258–265.
[4] Liochev, S.I. and Fridovich, I. (1997) Arch. Biochem. Biophys. 337, 115–120.
[5] Liochev, S.I. and Fridovich, I. (1995) Arch. Biochem. Biophys. 318, 408–410.
[6] Vásquez-Vivar, J., Hogg, N., Pritchard Jr., K.A., Martásek, P. and Kalyanaraman, B. (1997) FEBS Lett. 403, 127–130.
[7] Frey, C., Narayanan, K., McMillan, K., Speck, L., Gross, S.S., Masters, B.S. and Griffith, O.W. (1994) J. Biol. Chem. 269, 26083–26091.
[8] Benov, L., Sztejnberg, L. and Fridovich, I. (1998) Free Radic. Biol. Med. 25, 826–831.
[9] Vásquez-Vivar, J., Martásek, P., Hogg, N., Karoui, H., Masters, B.S.S., Pritchard Jr., K.A. and Kalyanaraman, B. (1998) Methods Enzymol. 301, 169–177.
[10] Finkelstein, E., Rosen, G.M. and Rauckman, E.J. (1982) Mol. Pharmacol. 21, 262–265.
[11] Fréjaville, C., Karoui, H., Tuccio, B., Le Moigne, F., Culcasi, M., Pietri, S., Laruicella, R. and Tordo, P. (1994) J. Chem. Soc. Chem. Commun., 1793–1794.
[12] Olive, G., Mercier, A., Le Moigne, L., Rockenbauer, A. and Tordo, P. (2000) Free Radic. Biol. Med., in press.
[13] Olive, G., Le Moigne, F., Mercier, A., Rockenbauer, A. and Tordo, P. (1998) J. Org. Chem. 63, 9095–9099.
[14] Kornblum, N., Blackwood, R.K. and Powers, J.W. (1957) J. Am. Chem. Soc. 79, 2507–2509.
[15] Bonnett, R., Brown, R.F.C., Clark, V.M., Sutherland, I.O. and Todd, A. (1959) J. Chem. Soc., 2094–2102.
[16] Vásquez-Vivar, J., Hogg, N., Martásek, P., Karoui, H., Pritchard Jr., K.A. and Kalyanaraman, B. (1999) J. Biol. Chem. 274, 26736–26742.
[17] Vásquez-Vivar, J., Kalyanaraman, B., Martásek, P., Hogg, N., Masters, B.S.S., Karoui, H., Tordo, P. and Pritchard Jr., K.A. (1998) Proc. Natl. Acad. Sci. USA 95, 9220–9225.
[18] Froncisz, W. and Hyde, J.S. (1982) J. Magn. Reson. 43, 515–521.
[19] Rockenbauer, A. and Korecz, C. (1996) Appl. Magn. Reson. 10, 29–43.
[20] Roubaud, V., Mercier, A., Olive, G., Le Moigne, F. and Tordo, P. (1997) J. Chem. Soc. Perkin Trans. II 2, 1827–1830.
[21] Karoui, H., Nsanzumuhire, C., Le Moigne, F. and Tordo, P. (1999) J. Org. Chem. 64, 1471–1477.
[22] Tordo, P. (1998) Electron Paramagn. Reson. 16, 116–144.
[23] Ohara, Y., Peterson, T.E. and Harrison, D.G. (1993) J. Clin. Invest. 91, 2546–2551.
[24] Harrison, D.G. (1997) J. Clin. Invest. 100, 2153–2157.
[25] Stroes, E.S.G., van Faasen, E.E., van Londen, G.J. and Rabelink, T.J. (1998) J. Cardiovasc. Pharmacol. 32 (Suppl. 3), S14–S21.
[26] Weaver, R.M.F., Lüscher, T.F., Cosentino, F. and Rabelink, T.J. (1998) Circulation 97, 108–112.
[27] Cosentino, F., Patton, S., d'Uscio, L.V., Werner, E.R., Werner-Felmayer, G., Moreau, P., Malinski, T. and Lüscher, T.F. (1998) J. Clin. Invest. 101, 1530–1537.
[28] Pritchard Jr., K.A., Groszek, L., Smalley, D.M., Sessa, W.C., Wu, M., Villon, P., Wolin, M.S. and Stemerman, M.B. (1995) Circ. Res. 77, 510–518.